Biosensors and Bioelectronics 130 (2019) 103–109

Contents lists available at ScienceDirect

Biosensors and Bioelectronics

journal homepage: www.elsevier.com/locate/bios

Development of a novel micro biosensor for *in vivo* monitoring of glutamate release in the brain

Mallikarjunarao Ganesana, Elefterios Trikantzopoulos, Yash Maniar, Scott T. Lee, B. Jill Venton*

Department of Chemistry and Neuroscience Graduate Program, University of Virginia, Charlottesville, VA, USA

ARTICLE INFO

Keywords:
Glutamate biosensor
Glutamate
In vivo
Stimulated glutamate and amperometry

ABSTRACT

L- Glutamate is the main excitatory neurotransmitter in the central nervous system and hyperglutamatergic signaling is implicated in neurological and neurodegenerative diseases. Monitoring glutamate with a glutamate oxidase-based amperometric biosensor offers advantages such as high spatial and high temporal resolution. However, commercially-available glutamate biosensors are expensive and larger in size. Here, we report the development of 50 μm diameter biosensor for real-time monitoring of L-glutamate *in vivo*. A polymer, poly-o-phenylenediamine (PPD) layer was electropolymerized onto a 50 μm Pt wire to act as a permselective membrane. Then, glutamate oxidase entrapped in a biocompatible chitosan matrix was cast onto the microelectrode surface. Finally, ascorbate oxidase was coated to eliminate interferences from high levels of extracellular ascorbic acid present in brain tissue. L-glutamate measurements were performed amperometrically at an applied potential of 0.6 V *vs* Ag/AgCl. The biosensor exhibited a linear range from 5 to 150 μM, with a high sensitivity of 0.097 ± 0.001 nA/μM and one-week storage stability. The biosensor also showed a rapid steady state response to L-glutamate within 2 s, with a limit of detection of 0.044 μM. The biosensor was used successfully to detect stimulated glutamate in the subthalamic nucleus in brain slices and *in vivo*. Thus, this biosensor is appropriate for future neuroscience applications.

1. Introduction

L-Glutamate is one of the most prevalent excitatory signaling molecules in the central nervous system (CNS) (Salazar et al., 2016) and plays a crucial role in a variety of brain functions such as memory and learning (Danbolt, 2001; Nedergaard et al., 2002). At elevated concentrations, glutamate exhibits excitotoxic properties that are implicated in a variety of neurological disorders including ischemic stroke (Camacho and Massieu, 2006), epilepsy (Babb et al., 1998), and neurodegenerative diseases (Mehta et al., 2013). Basal glutamate concentrations *in vivo* range from 0.9 to 3.7 μM (Day et al., 2006; Stephens et al., 2011; Vasylieva et al., 2013), however during pathological situations glutamate levels increase several fold (Wahl et al., 1994; Lee et al., 2009). Monitoring glutamate in real-time is key to understanding its normal and pathological functions. Traditionally, *in vivo* glutamate levels were monitored using microdialysis (Windels et al., 2000) but even the fastest measurements have a time resolution of only 15 s (Venton et al., 2006). Moreover, microdialysis probes cause significant damage to brain tissue due to the larger size, with a diameter from 200 to 500 μm and length of 1–4 mm (Hascup et al., 2009; Hascup and Hascup, 2014). Therefore, small sensors with a fast time response and large linear range are required to measure real-time glutamate release *in vivo*.

Glutamate is not electroactive and cannot be directly detected by voltammetry but enzyme-based electrochemical biosensors can monitor glutamate continuously (Hu et al., 1994; Özel et al., 2014; Vasylieva et al., 2013). Many glutamate biosensors utilize glutamate oxidase (GlutOx) to enable real-time glutamate measurements in the brain. GlutOx metabolizes glutamate and releases hydrogen peroxide, which is electroactive and can be detected electrochemically (Özel et al., 2014). GlutOx sensors are dependent on oxygen, but operate well at normoxic conditions (Clay and Monbouquette, 2018). Glutamate dehydrogenase has also been employed in biosensor applications and is not oxygen dependent; however, it has longer response times, lower sensitivity, and requires a NAD^+ cofactor (Hughes et al., 2016).

Several different glutamate biosensors have been developed in recent years. For physiological applications, enzymes are typically coated on platinum wire electrodes (Batra et al., 2016; Hu et al., 1994; Özel et al., 2014). Commercially available GlutOx-based biosensor designs are available (Pinnacle Technology, Inc. USA), but they are larger than

Abbreviations: PPD, poly-o-phenylenediamine; GlutOx, Glutamate oxidase; AsOx, Ascorbate oxidase

* Correspondence to: PO Box 400319, Charlottesville, VA 22904, USA.
E-mail address: jventon@virginia.edu (B.J. Venton).

https://doi.org/10.1016/j.bios.2019.01.049
Received 31 October 2018; Received in revised form 9 January 2019; Accepted 20 January 2019
Available online 30 January 2019
0956-5663/

optimal for small model organisms (176 μm in diameter). Polymer-based, flexible glutamate sensors were developed for *in vivo* applications (Weltin et al., 2014) with a sensing core of only 100 μm, but an overall width of 500 μm. Microelectrode arrays for glutamate were designed with individual sensors that are less than 100 μm in size, and multiple sensors in a single assembly allow measurements of different analytes in parallel (Tolosa et al., 2013; Wassum et al., 2008). However, the overall width of the sensor at the site of implantation is on the order of a millimeter. Gerhardt's group developed multisite ceramic microelectrodes for *in vivo* glutamate detection in rats and mice (Burmeister et al., 2002; Hascup et al., 2008; Rutherford et al., 2007). These microelectrode arrays are triangular in shape with an active site on the order of 50–150 μm, but the actual taper starts from 1 mm. A smaller design would not only minimize the tissue damage during biosensor implantation and removal, but also would allow more precise targeting of brain regions.

In this study, we developed a microelectrode that is only 50 μm in diameter for measuring glutamate *in vivo* and in brain slices. The biosensor design includes electrochemical deposition of PPD, immobilization of GlutOx entrapped in a chitosan matrix, and a layer of ascorbate oxidase. Analytical performance was tested *in vitro* and the electrodes exhibited excellent sensitivity and selectivity for glutamate. Electrodes were batch fabricated, which is important for making new, disposable sensors for *in vivo* use. The response time was fast (2 s) and the limit of detection (0.044 μM) was sufficient for *in vivo* measurements. The biosensor was tested for real-time measurement of glutamate release *in vivo* in the subthalamic nucleus as well as in brain slices.

2. Materials and methods

2.1. Materials

Platinum wire (50 μm diameter) and glass capillary tubes were obtained from A-M Systems (Sequim, WA, USA). Polyimide capillaries with inner diameter of 100 μm were obtained from Polymicro Technologies (Lisle, IL, USA). Silver conducting epoxy was obtained from MG Chemicals (Ontario, Canada) and 5-min epoxy was obtained from Devcon (OH, USA). Glutamate oxidase (GlutOx) (EC 1.4.3.11, 25 U/vial; from *E. coli*) was obtained from Cosmo Bio USA, Inc. (Carlsbad, California, USA). Ascorbate oxidase (AsOx) was obtained from Alfa Aesar (Haverhill, MA USA). Silver wire, acetic acid, L-ascorbic acid, uric acid, adenosine, dopamine, and serotonin hydrochloride were obtained from Acros Organics (NJ, USA). Chitosan from shrimp shells, o-phenylenediamine, albumin from bovine serum, L-glutamic acid, and D-glucose anhydrous were obtained from Sigma-Aldrich (St. Louis, MO, USA). Isothesia was obtained from Henry Schein. Sulfuric acid was obtained from Fisher Scientific (Fair Lawn, NJ, USA).

2.2. Fabrication of the biosensor

Platinum wire working electrodes were fabricated through a multistep process. For each electrode, the Pt-wire was cut into 4 cm length, and the Teflon coating was carefully removed with the aid of micro scissors. The Pt microelectrode was inserted into a 1.5 cm length of polyimide capillary and 2 mm length exposed for biosensing as a protruding tip. Then, 5-min nonconductive epoxy was applied to seal the Pt wire-polyimide capillary interface, and the epoxy was cured for 30 min at room temperature. A glass capillary tube was pulled into two capillaries with a glass microelectrode puller and then the sharp end was polished. The polyimide capillary was inserted into the polished end of the glass capillary, with 1 cm of the polyimide capillary protruding out. The polyimide capillary-glass capillary interface was sealed using 5-min epoxy. A 4 cm piece of copper wire with adhesive silver conductive epoxy was inserted into the other end of the glass capillary to form an electrical connection between the copper wire and the extended Pt wire inside the glass tube. Finally, a 5-min epoxy bubble was placed to form

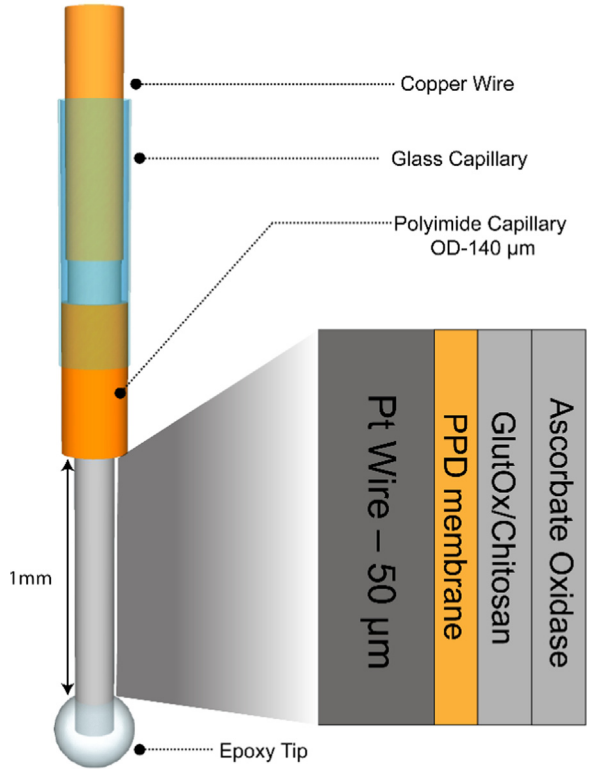

Fig. 1. Operational schematic of glutamate biosensor. The Pt wire is a 50 μm diameter and is coated with o-PD, GlutOx/Chitosan mixture, and AsOx. The wire has an epoxy tip at the protruding end to aid in enzyme deposition. The Pt wire is sheathed in a polyimide capillary (140 μm OD), which is subsequently inserted into a glass capillary tube. The top end of the Pt wire is connected to a copper wire *via* silver conducting epoxy; this copper wire makes contact with the potentiostat.

an epoxy tip on the exposed biosensing end of the Pt wire, such that 1 mm in length of the microelectrode was exposed (Fig. 1). This 1 mm protruding Pt wire excluding the epoxy bubble was the active biosensing surface, where enzymes were immobilized. The epoxy tip not only helps in loading the enzyme mixture on the sensor surface, but also prevents sensor from mechanical damage during implantation.

Next, the Pt wire microelectrodes were cleaned in 0.5 M sulfuric acid using cyclic voltammetry by scanning from -0.3 to 1.5 V at 100 mV/s for 20 cycles. After rinsing thoroughly with distilled water, the clean electrode was electrocoated with o-PD by applying a potential of + 0.7 V for 10 min in a stirred solution of 300 mM o-PD in PBS buffer at pH 7.4. This method produces a thin, perm-selective and self-sealing PPD film on the Pt surface to improve selectivity towards glutamate (Killoran and O'Neill, 2008). The electrodes were quickly rinsed with distilled water and immediately modified with a 1:2 ratio of 0.1 U/μL GlutOx in 0.1 M PBS (pH = 7.4) with 1% chitosan in 0.1 M acetic acid. Two aliquots of 1.5 μL mixture were manually deposited on the working area of the Pt wire and allowed to dry between each drop. Finally, 2 μL of 200 U/mL AsOx was manually deposited on to the electrode surface and allowed to dry. The prepared biosensors were then stored in a refrigerator until use. Prior to use, the electrode was dipped in 5 mg/mL bovine serum albumin for one minute to avoid non-specific adsorption.

2.3. In vitro calibration and characterization of the biosensor

Biosensors were first characterized *in vitro* to generate a standard calibration curve for conversion of glutamate current to concentration. Amperometry and cyclic voltammetry experiments were performed using a Reference 600 Potentiostat (Gamry Instruments, USA) with a modified Pt biosensor as the working electrode, a standard Ag/AgCl

reference electrode (3.5 mm O.D) (RRPEAGCL, Pine research, USA), and a 500 μm Pt wire as a counter electrode. Biosensor performance was characterized using amperometry at an applied potential of + 0.6 V *in vitro*. Calibrations were carried out in 5 mL PBS under constant stirring.

2.4. Animal experiments and glutamate measurements

All animal experiments were reviewed and approved by the Institutional Animal Care and Use Committee of the University of Virginia. Animal welfare was monitored daily by animal care staff. Male Sprague-Dawley rats (Charles River Laboratories, Wilmington, MA, USA) between 250 and 350 g were housed in 12/12 h light/dark cycles and fed *ad libitum* and provided environmental enrichment. Surgeries were performed in the morning, during the beginning of the light cycle. Experiments were performed in the lab while animals were anesthetized.

2.4.1. In Vivo experiments and surgery

Rats were anesthetized with 50% wt urethane (Sigma Aldrich) solution in saline (1.5 g/kg, i.p). The surgical site was shaved and 0.25 mL of bupivicaine (APP Pharmaceuticals, LLC; Schaumburg, IL, USA) was administered subcutaneously for local analgesia. After exposing the skull, holes were drilled for the placement of electrodes using a stereotaxic drill. Stimulated glutamate measurements were conducted in subthalamic nucleus (STN) using the coordinates (in mm from bregma): anterior-posterior (AP): -3.5, mediolateral (mL): + 2.4, and dorsoventral (DV): − 7.5-8.1. Both working and stimulating electrodes were placed in the same region 100 μm apart. The reference electrode, 100 μm Ag/AgCl wire was inserted on the contralateral side of the brain. The rat's body temperature was maintained at 37 °C using a heating pad with a thermistor probe (FHC, Bowdoin, ME, USA). Stimulated glutamate release was measured by applying stimulation pulse trains (500 μA, 30 or 50 pulses, 120 Hz), and the glutamate response was recorded in the subthalamic nucleus.

2.4.2. Brain slice experiments

Rats were anesthetized with isoflurane (Isothesia) and beheaded. Four hundred μm thick sagittal slices containing the target region, the subthalamic nucleus, were collected in oxygenated artificial cerebral spinal fluid (aCSF) (Pajski and Venton, 2010). Once collected, slices were heated in a water bath to 37 °C to equilibrate for at least 30 min. During experiments, oxygenated aCSF was perfused over the slice at 2 mL/min. A biphasic stimulating electrode was rested on top of the tissue on the STN (approximate coordinates 2.9 mm mediolateral, 7.6 mm dorsoventral, −3.5 mm anteroposterior). The working electrode was implanted between the prongs of the stimulating electrode about 500 μm away. It was implanted through the tissue to maximize the surface area of the electrode that is in direct contact with the tissue. The stimulation parameters were used from the previous study (Windels et al., 2000). In short, we applied pulse trains of 10–50 pulses at a frequency of 120 Hz, where each pulse was biphasic, 1 ms duration per phase.

3. Results

3.1. In vitro characterization of glutamate biosensors

An operational schematic of the glutamate biosensor is shown in Fig. 1. The perm-selective PPD membrane blocks interferences from most large compounds (Killoran and O'Neill, 2008), preserves the catalytic activity of the enzyme, and thus enhances the overall sensitivity and stability of the biosensor (Özel et al., 2014). GlutOx catalyzes the oxidation of glutamate, a reaction that produces electroactive hydrogen peroxide, which is detected amperometrically. In the CNS, biological media such as cerebrospinal fluid, serum, and brain homogenates are

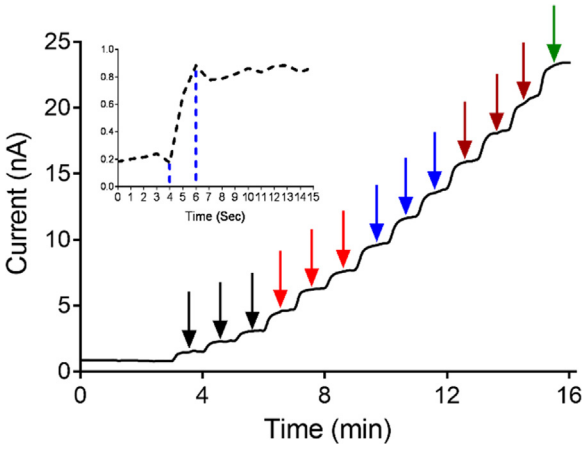

Fig. 2. Representative amperogram shows the biosensor response to glutamate. Applied potential is + 0.6 V vs Ag/AgCl. Arrows indicated with color coding are to indicate each of the individual concentrations tested in triplicate at 5 (black arrow), 10 (red arrow), 15 (blue arrow), and 20 μM (maroon arrow). Finally, one response to 25 μM (green arrow) is shown. Inset shows a response to 5 μM glutamate enlarged so that the time response can be seen. The sensor reaches its maximum in 2 s.

complex mixtures consisting of hundreds of biological molecules. Because ascorbate is one of the primary interferents in the central nervous system, at concentrations in the range of 200–400 μM (Miele and Fillenz, 1996), AsOx was also manually deposited to eradicate potential interference from ascorbic acid. Our biosensor design consists of a permselective PPD membrane, chitosan polymer matrix, both of which are known to reject ascorbic acid (Killoran and O'Neill, 2008; Özel et al., 2011; Sun et al., 2018). Moreover, chitosan is known to form thin films with a smooth surface without any visible pinholes on the micron scale, when mixed with enzymes (Tseng et al., 2013; Wei et al., 2002) or by itself (Özel et al., 2011). The biosensors were rinsed in bovine serum albumin prior to use to avoid non-specific adsorption of proteins during *in vivo* applications.

To characterize the biosensor, glutamate injections were performed in triplicate, starting at 5 μM and increasing in increments of 5 μM up until 50 μM. A representative amperogram is shown in Fig. 2. The biosensor has a fast response time and a steady state limiting current value was reached within 2 s (Fig. 2 inset). Thus, the polymer and enzymes layers are thin enough to allow a fast diffusion rate to the electrode surface. The range of concentrations tested were from 5 to 1500 μM glutamate (Fig. 3A) and the linear range was 5–150 μM (Fig. 3B). The sensitivity, the slope of the calibration curve, was 0.097 ± 0.001 nA/μM (n = 21). The limit of detection (LOD) was 0.044 μM and was calculated using the formula LOD = 3 * (SD/m) where SD = standard deviation of the amperometric signal of PBS, and m = slope of the calibration curve (Fig. 3B). The basal concentration of extracellular glutamate ranges from 1 to 5 μM (Mitani et al., 1992) and can increase up to 15-fold after ischemia, so the LOD and linear range are in the physiological range.

3.2. Biosensor selectivity and shelf life

To verify the specificity of the biosensor response to glutamate only, selectivity testing was conducted *in vitro* using common neurochemicals such as 100 nM serotonin, 1 μM adenosine, 1 μM dopamine, 0.5 mM glucose, 100 μM uric acid, and 200 μM ascorbic acid. The biosensor showed a negligible response to these analytes, indicating no interference (Fig. 4A). The current response to 20 μM glutamate was tested before and after the other analytes, and the biosensor did not show any change in current response to glutamate. These results also suggest that exposure to other neurochemicals does not affect the performance of

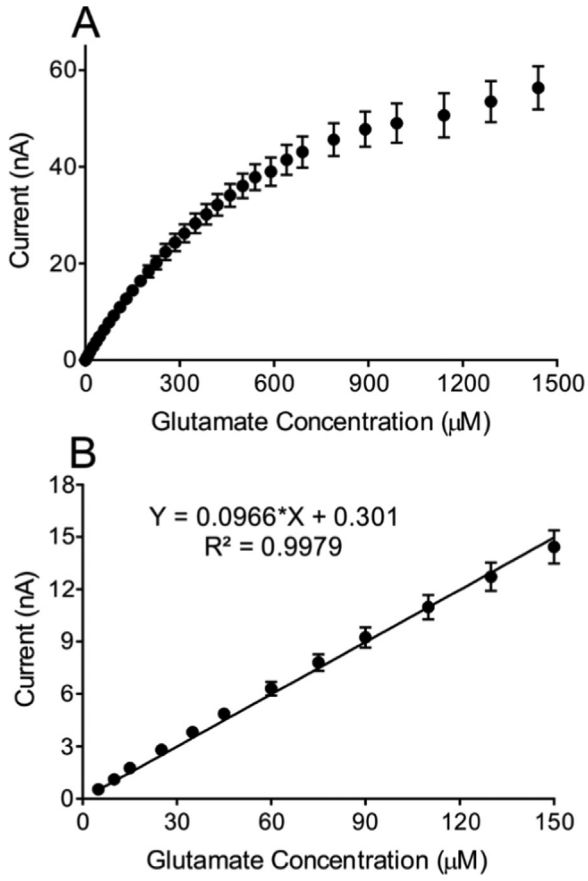

Fig. 3. (A) Glutamate biosensor calibration curve showing the sensor performance from 5 μM to 1500 μM glutamate. (B) Biosensor has a linear range up to 150 μM (n = 21). Within the linear range the biosensor reliably measures glutamate with a sensitivity of 0.097 nA/μM.

the biosensor and its sensitivity to glutamate.

For *in vivo* experiments measuring glutamate, it is important to be able to fabricate many biosensors at the same time reproducibly. To explore batch fabrication, we made many batches of sensors (typically 6–8 sensors per batch) and randomly selected some (n = 8) to create linear calibration curves. Fig. 4B shows the calibration curves of individual sensors from multiple batches as well as a few sensors from the same batch. Small variations between sensors are caused by varying length due to hand fabrication, as the enzyme loading, or polymer coatings might not be the same each time and could be improved in the future with a mass fabrication approach. The relative standard deviation of the calibration slope for sensors within the same batch is 8–18% and between multiple batches is about 34%, because there was likely variability in sensor size and enzyme activity. The data show that, overall these sensors were highly reproducible both between batches and within the same batch.

The storage stability of the biosensors was tested to monitor the shelf life of the sensors. The change in glutamate sensitivity was measured over a 7-day period, while biosensors were stored under dry conditions at + 4 °C. When sensors were tested daily for seven days (n = 5), they exhibited about 40% loss over a week, with only 10–15% losses over the first 2 days (Fig. 5A). Loss in sensitivity was likely due to repeated use, causing loss of adsorbed enzyme or enzyme activity. Some electrodes were tested on day 1 and then stored and then tested again on day 7. These electrodes (n = 7) showed only a 5% loss in signal on day 7 (Fig. 5B), suggesting that larger losses seen in the daily testing were due to multiple tests. Normally, *in vivo* sensors are only used one time; thus, these sensors can be made and initially verified and then can be stored for up to a week before they would be used for *in vivo* experiments.

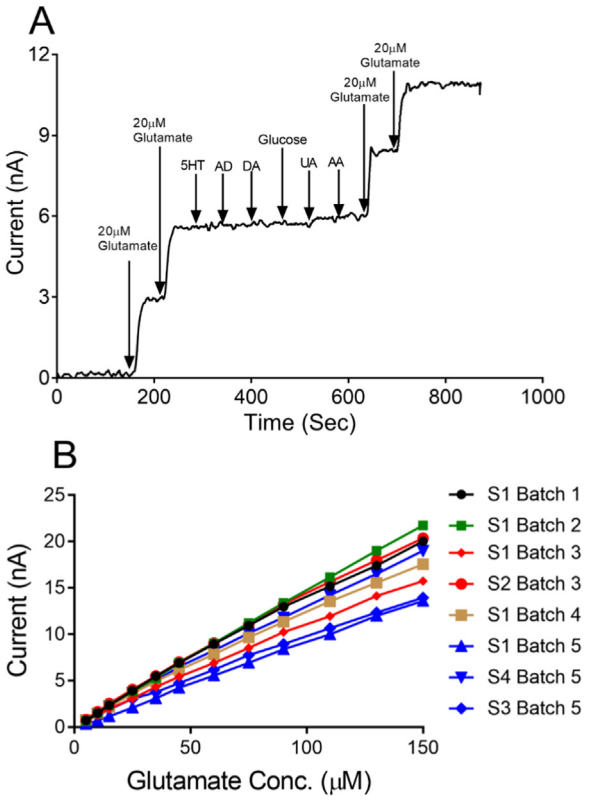

Fig. 4. (A) Glutamate biosensor *in vitro* selectivity testing. Following two injections of 20 μM glutamate, a series of common neurochemicals were injected to the electrochemical cell in order to ensure that the biosensor responds only to glutamate. The following species were used: 100 nM serotonin (5HT), 1 μM adenosine (AD), 1 μM dopamine (DA), 0.5 mM glucose, 100 μM uric acid (UA) and 200 μM ascorbic acid (AA). Current response to 20 μM glutamate prior to exposure to these interferents (0.135 nA/μM) did not change significantly afterwards (0.123 nA/μM). (B) Batch fabrication and comparison between batches. Glutamate biosensors fabricated in different batches were randomly selected and tested for the linear range (n = 8). Sensor fabrication is highly reproducible between batches and within a batch.

3.3. Comparison to other biosensors

Table 1 shows a comparison of different biosensors and their analytical performance characteristics for glutamate. Our sensor has comparable sensitivity to many sensors, with a low LOD and an extended linear range. The commercially available glutamate biosensor (Pinnacle Technology, Inc.) reports a linear range only up to 50 μM, which is smaller than our biosensor. Although 50 μM is sufficient for normal physiological glutamate levels (Hamdan and Zain, 2014), a larger linear range is necessary for *in vitro* cell culture studies and in disease models where glutamate is overstimulated. An example is a study using the commercial glutamate biosensor that measured glutamate after *in vivo* high frequency stimulation of the rat subthalamic nucleus, but found levels that were out of the linear range (Lee et al., 2007). Another advantage of our sensor is size, as biosensors are an invasive technique and some tissue injury upon implantation is inevitable. Our miniaturized biosensor, with a diameter of 50 μm, would minimize tissue damage and is overall smaller in total footprint than other *in vivo* biosensors. Future studies could also miniature our design even further, by making biosensors on the 20–30 μm scale. Because it is based on GlutOx, our sensor is oxygen dependent, and might not be suitable for low oxygen measurements. This limitation can be overcome by incorporation of nanoparticles that release oxygen or using glutamate

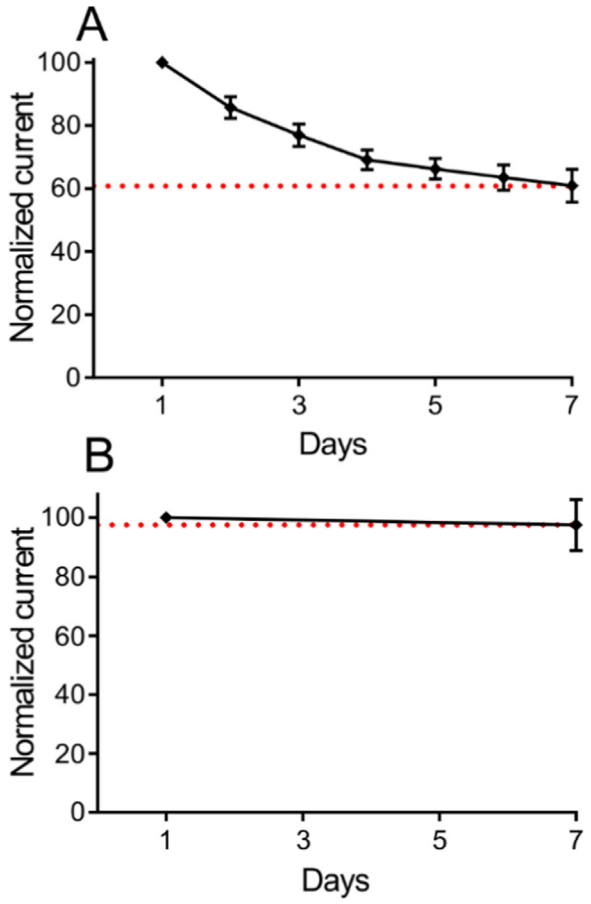

Fig. 5. Shelf life stability of glutamate biosensor. (A) The sensitivity of biosensors from Day 1 to Day 7 (Day 0 was the day of enzyme deposition). There was ~40% loss in average sensitivity (n = 5) from Day 1 to Day 7. (B) Biosensors tested on Day1 and Day 7 shows ~5% loss in average sensitivity (n = 7). In both studies, biosensors were stored under dry conditions at + 4 °C between the tests.

dehydrogenase (Hughes et al., 2016; Özel et al., 2014), but sensors based on GlutOx are faster and more sensitive and thus are the preferred strategy. Overall, our sensor had superior performance and size compared to previous sensors.

3.4. Application of the biosensor in rat brain slice and in vivo

To demonstrate the potential use of these biosensors for real-time biological applications, measurements of stimulated glutamate release were made in rat brain slices and *in vivo*. Electrodes were calibrated before and after tissue experiments and the response decreased, typical of most biosensors, but they were still functional *in vivo* (Fig. S1). Extracellular glutamate changes were measured during high frequency stimulation of the STN, since it is well known that as stimulation increases glutamate levels increases in that region (Lee et al., 2007). In rat brain slices, the sensor was first placed in the slice and a stable baseline established (~30 min) before applying the biphasic electrical stimulations of 10, 30, or 50 pulses. As shown in Fig. 6A, there was a pronounced increase in peak current right after the stimulation and higher numbers of stimulation pulses produced more glutamate. The initial downward spike after stimulation is due to electrical noise caused by the electrical stimulation. After the stimulation ends, extracellular glutamate concentration decreased back to pre-stimulus baseline levels, due to uptake and metabolism. Fig. 6B also shows the overlay of two current vs time responses to allow a direct comparison of electrically stimulated glutamate for 30 and 50 pulses in brain slice.

Biosensor performance *in vivo* was also tested in the STN of anesthetized rats by applying 30 or 50 pulse stimulations. The stimulation error *in vivo* was in the positive direction and the short spike after the stimulation is due to electrical noise from the electrical stimulation (Fig. 6C). However, the longer rise after the spike is the glutamate signal. Stimulated glutamate measurements were carried out over a 4-h period, with stimulations repeated every five minutes. Fig. 6C shows the overlay of electrically stimulated glutamate responses for 30 and 50 pulses taken at different time points.

The high-frequency stimulation in STN of rats is similar to deep brain stimulation in humans used for the treatment of disorders such as Parkinson's disease (Lozano et al., 2002). The major source of the increase in extracellular glutamate in STN during electrical stimulations is axonal stimulation of descending glutamatergic cortical inputs to the STN and axonal collaterals within the STN (Wilson et al., 2004). Stimulated glutamate levels were in the micromolar range and our sensor could detect and quantify them with high reproducibility and fast temporal resolution. Our levels of stimulated glutamate release match with previous reports of 3–20 μM and release was easily detected at our biosensor (Lee et al., 2007, 2004). Moreover, the stable response of biosensor even after 4 h of implantation is useful for longer experiments in the future that involve pharmacology or disease pathology. The *in vivo* measurements in both brain slices and intact rat brains demonstrate these biosensors could be useful for investigating the role of real-time glutamate signaling in many diseases.

4. Conclusions

We developed a glutamate biosensor with chitosan as a matrix for the immobilization of the enzyme glutamate oxidase on the surface of a platinum electrode. Our miniaturized biosensor of 50 μm in diameter can be applied for monitoring glutamate *in vivo* and in brain slices. The biosensor exhibited high sensitivity, while rejecting interferences, with a fast response time (~2 s) and a linear range of 5–150 μM. Biosensors were stable for 7 days when stored dry at + 4 °C and had good reproducibility within a batch and between batches. Stimulated glutamate release was successfully measured both in brain slices and *in vivo*. This biosensor has the potential to directly monitor glutamate *in vivo* with minimal tissue damage. Future studies can test the long-term operational and storage stability of the sensor and its viability in long-term *in vivo* applications. Small variations of length between sensors due to hand fabrication could be improved in future with a mass fabrication approach.

Table 1
Comparison of different biosensors configurations and their analytical performance characteristics for glutamate.

Electrode configuration	Sensitivity	Linear range	LOD	Response time	References
Pt-Ir/Mixed ceria and titania nanoparticles	793 pA/μM	5–50 μM	0.6 μM	~5 s	(Özel et al., 2014)
Pt-Ir/Nafion/Poly(o-phenylenediamine)/GlutOx/poly(ethylene glycol) diglycidyl ether	14.6 pA/μM	20–100 μM	1 μM	~3.4 s	(Sirca et al., 2014)
Pt-disc/PEI/GlutOx/PPD-BSA	71 nA/μM	5–50 μM	2.5 μM	~5 s	(Govindarajan et al., 2013)
Pt microelectrode array /PPy/Nafion/GlutOx	2.46 pA/μM	10–100 μM	< 1 μM	< 1 s	(Wassum et al., 2008)
Pt-Ir/PPD/GlutOx/AscOx/BSA	97 pA/μM	5–150 μM	0.044 μM	~2 s	This Study

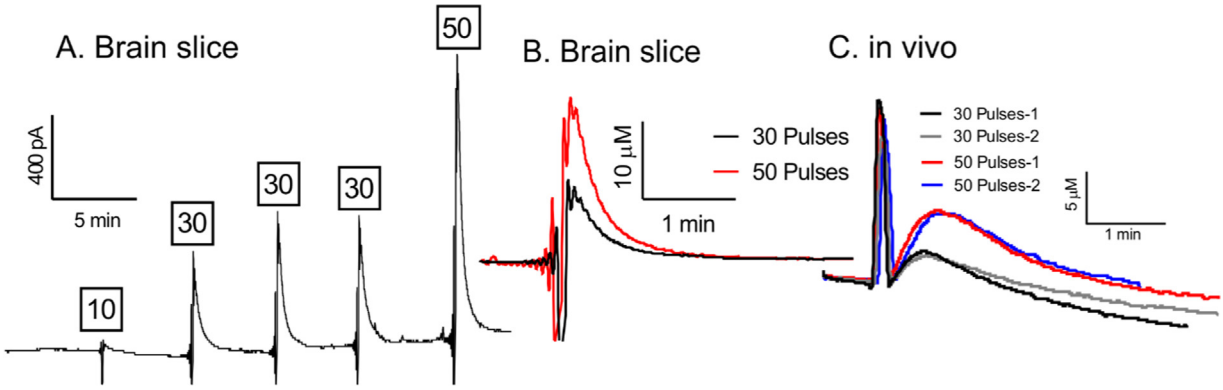

Fig. 6. Stimulated glutamate data in rat subthalamic nucleus brain slice and *in vivo*. (A) Representative amperogram of stimulated glutamate release in the subthalamic nucleus of a rat brain slice. The tissue was stimulated five times with a frequency of 120 Hz and pulse numbers are given above each stimulation. (B) Overlay of concentration vs time curves, allowing for comparison of 30 and 50 pulse stimulations. Sharp downward spike prior to peak glutamate response is electrical noise due to electrical stimulation. (C) *In vivo*, the rat brain was stimulated four times with a frequency of 120 Hz. Depicted here are two 30 pulse and two 50 pulse stimulations overlaid as concentration vs time curves, showing stability. Sharp spike prior to peak glutamate response is electrical noise due to electrical stimulation.

Acknowledgments

This work was funded by NIH (National Institue of Health, USA) under grants R01NS076875 and R01EB026497 to BJV.

Conflict of interest

The Authors have no conflict of interest.

Credit author statement

B. Jill Venton was involved in conceptualization, funding acquisition, project administration, resources, supervision, writing original draft, review, and editing. Mallikarjunarao Ganesana involved in conceptualization, methodology, data acquisition and curation, project administration, supervision, validation, writing original draft, review and editing. Elefterios Trikantzopoulos was involved in conducting experiments, methodology and data aquisition, and curation. Yash Maniar was involved in conducting experiments, data aquisition and curation. Scott T. Lee was involved in conducting experiments.

Appendix A. Supplementary material

Supplementary data associated with this article can be found in the online version at https://doi.org/10.1016/j.bios.2019.01.049.

References

Babb, T.L., Ying, Z., Hadam, J., Penrod, C., 1998. Glutamate receptor mechanisms in human epileptic dysplastic cortex. Epilepsy Res. 32, 24–33. https://doi.org/10.1016/S0920-1211(98)00037-0.

Batra, B., Yadav, M., Pundir, C.S., 2016. l-Glutamate biosensor based on l-glutamate oxidase immobilized onto ZnO nanorods/polypyrrole modified pencil graphite electrode. Biochem. Eng. J. 105, 428–436. https://doi.org/10.1016/j.bej.2015.10.012.

Burmeister, J.J., Pomerleau, F., Palmer, M., Day, B.K., Huettl, P., Gerhardt, G.A., 2002. Improved ceramic-based multisite microelectrode for rapid measurements of L-glutamate in the CNS. J. Neurosci. Methods 119, 163–171. https://doi.org/10.1016/S0165-0270(02)00172-3.

Camacho, A., Massieu, L., 2006. Role of glutamate transporters in the clearance and release of glutamate during ischemia and its relation to neuronal death. Arch. Med. Res. 37, 11–18. https://doi.org/10.1016/j.arcmed.2005.05.014.

Clay, M., Monbouquette, H.G., 2018. A detailed model of electroenzymatic glutamate biosensors to aid in sensor optimization and in applications in vivo. ACS Chem. Neurosci. 9, 241–251. https://doi.org/10.1021/acschemneuro.7b00262.

Danbolt, N.C., 2001. Glutamate uptake. Prog. Neurobiol. 65, 1–105. https://doi.org/10.1016/S0301-0082(00)00067-8.

Day, B.K., Pomerleau, F., Burmeister, J.J., Huettl, P., Gerhardt, G.A., 2006. Microelectrode array studies of basal and potassium-evoked release of l-glutamate in the anesthetized rat brain. J. Neurochem. 96, 1626–1635. https://doi.org/10.1111/j.1471-4159.2006.03673.x.

Govindarajan, S., McNeil, C.J., Lowry, J.P., McMahon, C.P., O'Neill, R.D., 2013. Highly selective and stable microdisc biosensors for l-glutamate monitoring. Sens. Actuators B Chem. 178, 606–614. https://doi.org/10.1016/j.snb.2012.12.077.

Hamdan, S.K., Zain, Z.M., 2014. In vivo electrochemical biosensor for brain glutamate detection: a mini review. Malays. J. Med. Sci. 21, 11–25.

Hascup, E.R., af Bjerkén, S., Hascup, K.N., Pomerleau, F., Huettl, P., Strömberg, I., Gerhardt, G.A., 2009. Histological studies of the effects of chronic implantation of ceramic-based microelectrode arrays and microdialysis probes in rat prefrontal cortex. Brain Res. 1291, 12–20. https://doi.org/10.1016/j.brainres.2009.06.084.

Hascup, K.N., Hascup, E.R., 2014. Electrochemical techniques for subsecond neurotransmitter detection in live rodents. Comp. Med. 64, 249–255.

Hascup, K.N., Hascup, E.R., Pomerleau, F., Huettl, P., Gerhardt, G.A., 2008. Second-by-second measures of L-Glutamate in the prefrontal cortex and striatum of freely moving mice. J. Pharmacol. Exp. Ther. 324 (725), . (LP-731).

Hu, Y., Mitchell, K.M., Albahadily, F.N., Michaelis, E.K., Wilson, G.S., 1994. Direct measurement of glutamate release in the brain using a dual enzyme-based electrochemical sensor. Brain Res. 659, 117–125. https://doi.org/10.1016/0006-8993(94)90870-2.

Hughes, G., Pemberton, R.M., Fielden, P.R., Hart, J.P., 2016. The design, development and application of electrochemical glutamate biosensors. TrAC Trends Anal. Chem. 79, 106–113. https://doi.org/10.1016/j.trac.2015.10.020.

Killoran, S.J., O'Neill, R.D., 2008. Characterization of permselective coatings electrosynthesized on Pt–Ir from the three phenylenediamine isomers for biosensor applications. Electrochim. Acta 53, 7303–7312. https://doi.org/10.1016/j.electacta.2008.03.076.

Lee, G.J., Choi, S.K., Kang, S.W., Choi, S., Park, J.H., Park, D.H., Park, Y.H., Kim, K.S., Park, H.K., 2009. Real-Time Monitoring of Extracellular Glutamate Release on Repetitive Ischemic Injury in Global Ischemia Model BT. In: Dössel, O., Schlegel, W.C. (Eds.). World Congress on Medical Physics and Biomedical Engineering, September 7 - 12, 2009, Munich, Germany. Springer Berlin Heidelberg, Berlin, Heidelberg, pp. 835–837.

Lee, K.H., Chang, S.-Y., Roberts, D.W., Kim, U., 2004. Neurotransmitter release from high-frequency stimulation of the subthalamic nucleus. J. Neurosurg. 101, 511–517. https://doi.org/10.3171/jns.2004.101.3.0511.

Lee, K.H., Kristic, K., van Hoff, R., Hitti, F.L., Blaha, C., Harris, B., Roberts, D.W., Leiter, J.C., 2007. High-frequency stimulation of the subthalamic nucleus increases glutamate in the subthalamic nucleus of rats as demonstrated by in vivo enzyme-linked glutamate sensor. Brain Res. 1162, 121–129. https://doi.org/10.1016/j.brainres.2007.06.021.

Lozano, A.M., Dostrovsky, J., Chen, R., Ashby, P., 2002. Deep brain stimulation for Parkinson's disease: disrupting the disruption. Lancet Neurol. 1, 225–231. https://doi.org/10.1016/S1474-4422(02)00101-1.

Mehta, A., Prabhakar, M., Kumar, P., Deshmukh, R., Sharma, P.L., 2013. Excitotoxicity: bridge to various triggers in neurodegenerative disorders. Eur. J. Pharmacol. 698, 6–18. https://doi.org/10.1016/j.ejphar.2012.10.032.

Miele, M., Fillenz, M., 1996. In vivo determination of extracellular brain ascorbate. J. Neurosci. Methods 70, 15–19. https://doi.org/10.1016/S0165-0270(96)00094-5.

Mitani, A., Andou, Y., Kataoka, K., 1992. Selective vulnerability of hippocampal CA1 neurons cannot be explained in terms of an increase in glutamate concentration during ischemia in the gerbil: brain microdialysis study. Neuroscience 48, 307–313. https://doi.org/10.1016/0306-4522(92)90492-K.

Nedergaard, M., Takano, T., Hansen, A.J., 2002. Beyond the role of glutamate as a neurotransmitter. Nat. Rev. Neurosci. 3, 748.

Özel, R.E., Wallace, K.N., Andreescu, S., 2011. Chitosan coated carbon fiber microelectrode for selective in vivo detection of neurotransmitters in live zebrafish embryos. Anal. Chim. Acta 695, 89–95. https://doi.org/10.1016/j.aca.2011.03.057.

Özel, R.E., Ispas, C., Ganesana, M., Leiter, J.C., Andreescu, S., 2014. Glutamate oxidase biosensor based on mixed ceria and titania nanoparticles for the detection of glutamate in hypoxic environments. Biosens. Bioelectron. 52, 397–402. https://doi.org/10.1016/j.bios.2013.08.054.

Pajski, M.L., Venton, B.J., 2010. Adenosine release evoked by short electrical stimulations in striatal brain slices is primarily activity dependent. ACS Chem. Neurosci. 1, 775–787. https://doi.org/10.1021/cn100037d.

Rutherford, E.C., Pomerleau, F., Huettl, P., Strömberg, I., Gerhardt, G.A., 2007. Chronic second-by-second measures of l-glutamate in the central nervous system of freely moving rats. J. Neurochem. 102, 712–722. https://doi.org/10.1111/j.1471-4159.2007.04596.x.

Salazar, P., Martín, M., O'Neill, R.D., González-Mora, J.L., 2016. Glutamate microbiosensors based on Prussian Blue modified carbon fiber electrodes for neuroscience applications: in-vitro characterization. Sens. Actuators B Chem. 235, 117–125. https://doi.org/10.1016/j.snb.2016.05.057.

Sirca, D., Vardeu, A., Pinna, M., Diana, M., Enrico, P., 2014. A robust, state-of-the-art amperometric microbiosensor for glutamate detection. Biosens. Bioelectron. 61, 526–531. https://doi.org/10.1016/j.bios.2014.04.054.

Stephens, M.L., Quintero, J.E., Pomerleau, F., Huettl, P., Gerhardt, G.A., 2011. Age-related changes in glutamate release in the CA3 and dentate gyrus of the rat hippocampus. Neurobiol. Aging 32, 811–820. https://doi.org/10.1016/j.neurobiolaging.2009.05.009.

Sun, Q., Qian, B., Uto, K., Chen, J., Liu, X., Minari, T., 2018. Functional biomaterials towards flexible electronics and sensors. Biosens. Bioelectron. 119, 237–251. https://doi.org/10.1016/j.bios.2018.08.018.

Tolosa, V.M., Wassum, K.M., Maidment, N.T., Monbouquette, H.G., 2013. Electrochemically deposited iridium oxide reference electrode integrated with an electroenzymatic glutamate sensor on a multi-electrode arraymicroprobe. Biosens. Bioelectron. 42, 256–260. https://doi.org/10.1016/j.bios.2012.10.061.

Tseng, T.T.-C., Yao, J., Chan, W.-C., 2013. Selective enzyme immobilization on arrayed microelectrodes for the application of sensing neurotransmitters. Biochem. Eng. J. 78, 146–153. https://doi.org/10.1016/j.bej.2013.04.019.

Vasylieva, N., Maucler, C., Meiller, A., Viscogliosi, H., Lieutaud, T., Barbier, D., Marinesco, S., 2013. Immobilization method to preserve enzyme specificity in biosensors: consequences for brain glutamate detection. Anal. Chem. 85, 2507–2515. https://doi.org/10.1021/ac3035794.

Venton, B.J., Robinson, T.E., Kennedy, R.T., Maren, S., 2006. Dynamic amino acid increases in the basolateral amygdala during acquisition and expression of conditioned fear. Eur. J. Neurosci. 23, 3391–3398. https://doi.org/10.1111/j.1460-9568.2006.04841.x.

Wahl, F., Obrenovitch, T.P., Hardy, A.M., Plotkine, M., Boulu, R., Symon, L., 1994. Extracellular glutamate during focal cerebral ischaemia in rats: time course and calcium dependency. J. Neurochem. 63, 1003–1011. https://doi.org/10.1046/j.1471-4159.1994.63031003.x.

Wassum, K.M., Tolosa, V.M., Wang, J., Walker, E., Monbouquette, H.G., Maidment, N.T., 2008. Silicon wafer-based platinum microelectrode array biosensor for near real-time measurement of glutamate in vivo. Sensors 8, 5023–5036. https://doi.org/10.3390/s8085023.

Wei, X., Cruz, J., Gorski, W., 2002. Integration of enzymes and electrodes: spectroscopic and electrochemical studies of chitosan–enzyme films. Anal. Chem. 74, 5039–5046. https://doi.org/10.1021/ac020216e.

Weltin, A., Kieninger, J., Enderle, B., Gellner, A.-K., Fritsch, B., Urban, G.A., 2014. Polymer-based, flexible glutamate and lactate microsensors for in vivo applications. Biosens. Bioelectron. 61, 192–199. https://doi.org/10.1016/j.bios.2014.05.014.

Wilson, C.L., Puntis, M., Lacey, M.G., 2004. Overwhelmingly asynchronous firing of rat subthalamic nucleus neurones in brain slices provides little evidence for intrinsic interconnectivity. Neuroscience 123, 187–200. https://doi.org/10.1016/j.neuroscience.2003.09.008.

Windels, F., Bruet, N., Poupard, A., Urbain, N., Chouvet, G., Feuerstein, C., Savasta, M., 2000. Effects of high frequency stimulation of subthalamic nucleus on extracellular glutamate and GABA in substantia nigra and globus pallidus in the normal rat. Eur. J. Neurosci. 12, 4141–4146. https://doi.org/10.1046/j.1460-9568.2000.00296.x.